Draft version May 10, 2020
Typeset using LaTeX default style in AASTeX63

Analysis of the Evolution of the Milky Way and M31 Galaxy Merger Before Final Coalescence Through Surface Brightness Profiles

Michael Klein[1]

[1]*Steward Observatory 933 North Cherry Avenue Tucson, AZ 85721-0065*

(Dated: May 7, 2020)

ABSTRACT

The movement of stars throughout a galactic merger can be visualized through a plot that measures the apparent brightness versus the radius of a galaxy. The plot that is created with these two measurements is known as a surface brightness profile. With the surface brightness profile astronomers can see how the density of stars within a galaxy change with radius of the galaxy especially, during a major merger event. In this paper, we explore approximately 10 billion years of merging between the Milky Way and Andromeda galaxies. We take advantage of N-body simulations of the merging event over the next 10 billion years and find that the surface brightness profiles agree with the findings in van der Marel et al. (2012) which we then apply a Sersic fit to compare models with the simulation data. Although the results were calculated using elliptical galactic models instead of spiral galactic models, we found that the resulting data agreed relatively well with the findings in van der Marel et al. (2012).

Keywords: Local Group, Stellar Disk, Stellar Bulge, Major Merger, Spiral Galaxy, Elliptical Galaxy, Surface Brightness Profile

1. INTRODUCTION

The Andromeda Galaxy (M31) is at a distance of 770 kpc from the Milky Way (Ribas et al. 2005). In 2012 it was determined, with some certainty, that the Milky Way and M31 would eventually merge in about 4 Gyr (van der Marel et al. 2012). These two galaxies can be divided into 3 sections: bulge, disk, and halo. The bulge is a tightly packed group of stars within some larger structure. With respect to the Milky Way and M31 it refers to the central group of stars found around the center of each galaxy. The disk is the flat circular region of a galaxy that extends outward from the central bulge, for spiral galaxies the disk contains the spiral arms. The final component, the halo, is a roughly spherical extension of a galaxy that goes beyond the visible bulge and disk components. Contained within the galactic halo is the dark matter halo, which is itself an extension of the visible components of the galaxy and contains the distribution of dark matter around the galaxy. This paper is only interested in the visible components, the bulge and the disk. In both the bulge and the disk, as a result of decreasing density of stars, the measured surface brightness falls with increasing radius. These two properties can be fit to create what is known as a surface brightness profile. Throughout this paper we use concentration of light and light density interchangeably, however they mean the same thing in respects to this paper.

We can define a galaxies components by fitting a surface brightness profile with a Sersic profile. For instance, in Querejeta et al. (2015) they found that it was difficult to distinguish between ellipticals and face-on lenticulars (galaxy whose appearance is intermediate between elliptical and spiral galaxies) so they confirmed the morphological classification by analysing the surface brightness profile obtained from the galaxies. In Figure 1 Querejeta et al. (2015) uses surface brightness profiles to help distinguish between elliptical and face-on lenticular or S0 galaxies. Similar uses of the surface brightness profile can be used to determine the structure of both the disk and bulge of the Milky Way and M31 throughout the merger sequence. Specifically, it can show where the most densely concentrated area of stars is within the galaxies during the sequence.

Surface brightness profiles can be used in bulge classification. Galactic bulges are typically divided into two types: classical and pseudobulges. Classical bulges are more spherically symmetric and have older stellar populations whereas pseudobulges have more disk-like features (Brooks & Christensen 2016). A classical bulge can be observed when fitting

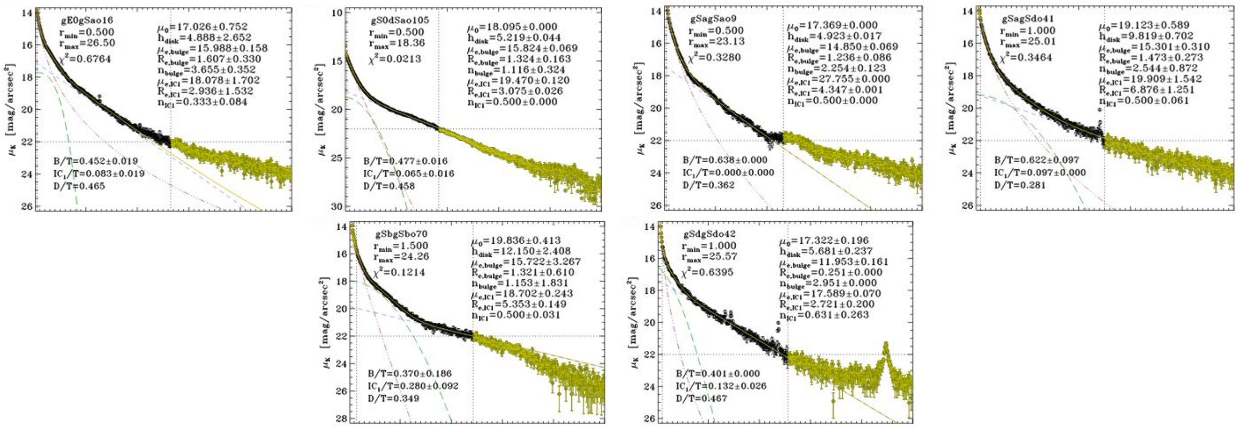

Figure 1: Figure 2 from Querejeta et al. (2015). Surface brightness profiles of some S0-like remnants from their observations. They used surface brightness profiles to determine whether these S0-like remnants were ellipticals or S0's. The black dots were included and the green empty dots were excluded from their data set. The red dotted dashed line is a fitted Sersic bulge and the blue dashed line is a fitted exponential disk. The green long dashed line was additional Sersic component required in their fit.

the surface brightness profile of the unknown bulge to a Sersic profile where the Sersic index, n, is equal to or greater than 2 (Brooks & Christensen 2016). A pseudobulge is observed when the surface brightness profile is fitted and compares well with a Sersic profile with n less than or equal to 2 (Brooks & Christensen 2016). The Milky Way is believed to have a boxy/peanut-shaped pseudobulge (Kormendy & Bender 2019) while M31 is said to have a classical bulge with pseudobulge trimmings (Mould 2013). The Sersic index is also used as an indication of whether the object is an elliptical galaxy or if it is a spiral galaxy, where an index of n = 4 is used for elliptical galaxies and an index of n = 1 is used for spiral galaxies (Trujillo et al. 2001).

It is relatively well understood that the concentration of most of the light that comes from a galaxy is centrally located, which is enforced by the exponential fit done to surface brightness profiles. The further an observer goes from the center, the less light is received by an observer. This is also seen in Figure 1 where the measured brightness decreases with radius from the center. However, what is less understood is how the variation in brightness changes throughout a merger sequence. It is not known whether the concentration of stars will move outward as the two galaxies get close enough to one another where tidal forces begin to throw stars out of each system. In van der Marel et al. (2012) they explain what the fate of our Sun might be because of this major merging event. More information on how the concentration of stars move throughout the event, may help identify the fate of the Sun.

2. THIS PROJECT

In this paper, we will investigate how the surface brightness profile of both the Milky Way and M31 will change as the two galaxies begin to move closer and start merging. Using N-body simulations of the Milky Way and M31 galaxies, we will investigate how the concentration of light changes throughout the merger sequence, stopping before final coalescence when the merger remnant resembles an elliptical galaxy (van der Marel et al. 2012).

We speculate that this study should provide a powerful indicator of how the two galaxies change with respect to the density of light and how it changes within both galaxies over billions of years. We will take advantage of N-body simulations of both the Milky Way and M31 galaxies to create our surface brightness profiles of both the bulge and disk. By utilizing the N-body simulations we can apply the de Vaucouleurs' Law which describes how surface brightness for an elliptical galaxy changes as a function of radius. With the de Vaucouleurs' Law we create a surface brightness profile and fit Sersic profiles to see if the models match with the simulation data.

Knowing how the concentrations of light or the stars within a galaxy move throughout a major merger event may help further improve other simulations of major mergers in the future. Understanding the question of how the stars will move throughout the merger sequence might also shed light on what the future of our own solar system is. After all, the Sun is one of the trillions of stars that would be a part of the merger event.

3. METHODOLOGY

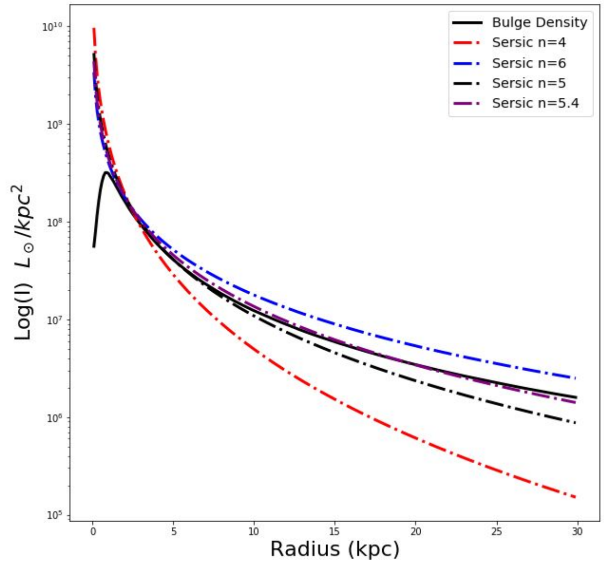

Figure 2: Example of a surface brightness profile. The solid black line is the surface brightness of the simulated bulge for M31. The various colored long dashed dotted lines are fitted Sersic profiles with indicated Sersic indices labelled n. The Sersic profile with index n=5.4 best fits the simulated bulge profile for this example.

We will take advantage of N-body simulations taken from van der Marel et al. (2012) of both the Milky Way and M31 galaxies to create our surface brightness profiles. An N-body simulation refers to a simulation of a gravitational system of particles that make up three or more massive bodies, where the gravitational system of particles represents either stellar or dark matter that makes up the bodies. The N-body simulation conducted in van der Marel et al. (2012) contained a collisionless aspect which means the particles did not interact with each other through collisions such as bouncing off one another. Instead, the particles interacted only through gravity and nothing else. This simulation took the three most massive galaxies of the Local Group (Milky Way, M31, and M33) and simulated their interactions over a period of approximately 11.5 Gyr, during which the Milky Way and M31 galaxies were shown to collide and eventually merge.

Our approach to studying the density of light contained within both the bulge and disk of the Milky Way and M31 is to use the simulation data obtained from van der Marel et al. (2012). We will observe how the surface brightness for both the bulge and disk changes and present snapshots of significant periods in which obvious changes to the profile occurs. The analysis will be very similar to what is shown in Figure 2. However, it will be more detailed and contain both the Milky Way and M31 with the fitted Sersic profiles that closely match the curve obtained of both the bulge and disk.

The first step in our analysis is to create an instance of the mass profile for the Milky Way and M31. We will use the mass profile to obtain the mass enclosed within the bulge and disk of the Milky Way and M31 out to a distance of 30 kpc. We chose 30 kpc because this was the upper limit for the radius of the Milky Way and M31 used in van der Marel et al. (2012). With both the disk and bulge mass enclosed we calculated the density profile using $I = L/(4\pi r^2)$ and we also assume a mass-to-light ratio of about 1 because we are using de Vaucouleurs' Law for elliptical galaxies. I is the apparent brightness, L is the same as mass enclosed since M/L=1 and r is the radius from the center (r = 0 kpc) to 30 kpc. We also need to compute the half-mass radius, where the half-mass radius is the radius at which half the mass is located. This was calculated by dividing the mass by 2. With these values we then calculated the Sersic fits to be applied to the plot by utilizing the Sersic profile in terms of effective radius or half-mass radius R_e: $I(r) = I_e exp[-7.67((r/R_e)^{1/n} - 1]$ where I_e is the effective intensity, r is the array of radii (0 to 30 kpc) and n is the Sersic index. This process will be done using the simulation data from van der Marel et al. (2012) to apply the process over time and will take snapshots of significant changes stopping before final coalescence or t = 10 Gyr which corresponds with the findings in van der Marel et al. (2012) when the merger remnant resembles an elliptical galaxy.

Once the correct equations are used and the information from the N-body simulations are applied, a graph of the apparent brightness versus the radius can be created. The long dashed dotted colored lines will be used to describe the Sersic fits that we fit to the resulting surface brightness calculations for both the Milky Way and M31 bulge and disk. The graphs will be a measure of both the surface brightness plotted on the y-axis versus the radius from the center of the galaxy plotted on the x-axis. We would then do the same thing for several more instances over the 10 Gyr time-span explained in the previous paragraph to observe how the concentration of light changes throughout the merger sequence.

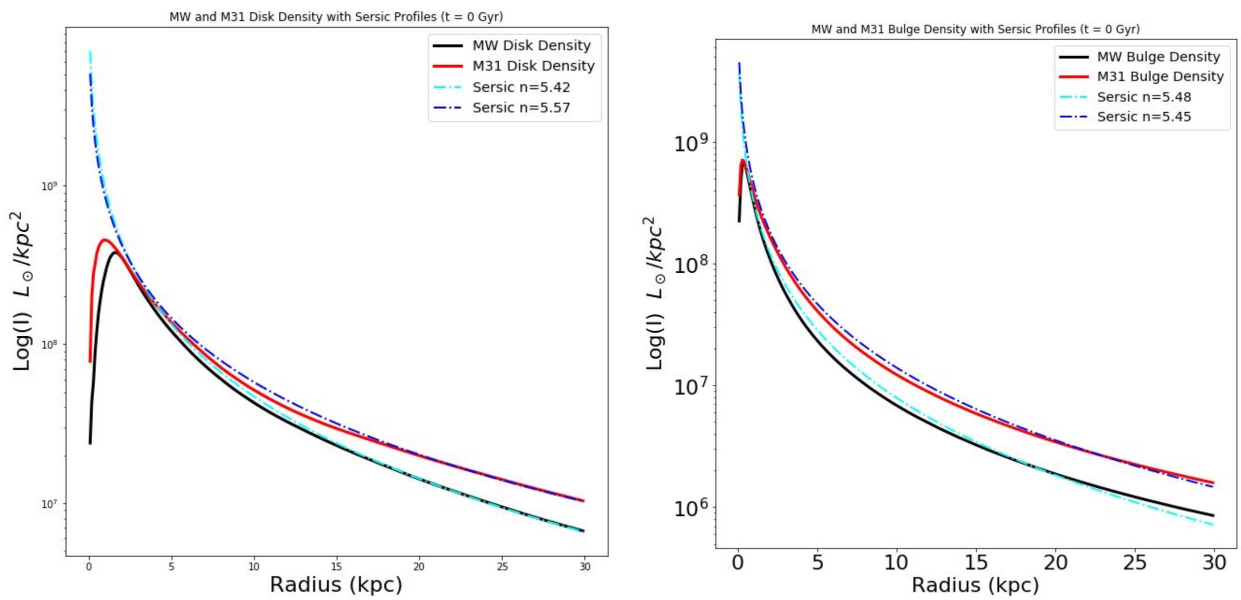

Figure 3: Surface brightness profiles of both the Milky Way and M31 galaxies at current day (t = 0 Gyr). The black and red solid lines describe the profiles created for both galaxies, where the peaks represent the most concentration of light. It can be seen that the most concentration of light appears to be closer to the center of both galaxies and falls off further from the center. The Sersic fits are described by the cyan and blue long dashed dotted lines with Sersic indices described with the n-values. The x-axis represents the radius from the center in kpc and the y-axis represents the apparent brightness.

We predict as the two galaxies begin to interact with one another gravitationally, we will see that the surface brightness will certainly match for points in the sequence when both bulges or both disks pass through one another. For instance, in Figure 3 we see that the disk densities for both galaxies are fairly equal with M31 having slightly more light density than the Milky Way and the bulge densities being fairly equal at close radii. We suspect that the concentration of stars will become more spread out as the two galaxies begin interacting and through fly-by's suggested in van der Marel et al. (2012). The graphs will show broader density distributions than what we see today as a result of the interactions.

4. RESULTS

Figure 3 displays our surface brightness profile for the current year and Figure 4 displays our surface brightness profiles for important moments during the merger sequence before final coalescence. Each profile was created using the methods discussed in section 3. All data was taken using the de Vaucouleurs' Law for elliptical galaxies and not the standard profiles for disk and bulge. Although the surface density profile calculated using de Vaucouleurs' Law would be the same for the bulge since the bulge resembles an elliptical galaxy as shown in Brooks & Christensen (2016).

In Figure 4 the first two graphs (upper left and upper middle) features a brightness profile that closely resembles the profile created of the current day Milky Way and M31 galaxies in Figure 3. However, there is visible disruption to the concentration of light with the disk, as we see that M31 appears to have lost some stars to the Milky Way, which has in turn increased in apparent brightness. Interestingly, the bulges appear to remain relatively unharmed. The second two graphs (upper right and middle left) feature the resulting fly-by of the two galaxies, although the distribution of light appears to be unchanged in the disk, the bulge has obvious broadening, most likely as a result of the close encounter. These two graphs represent right before the first Milky Way and M31 apocenter, or the furthest point from the center of attraction. The third set of graphs (middle middle and middle right) feature clear light density disruption

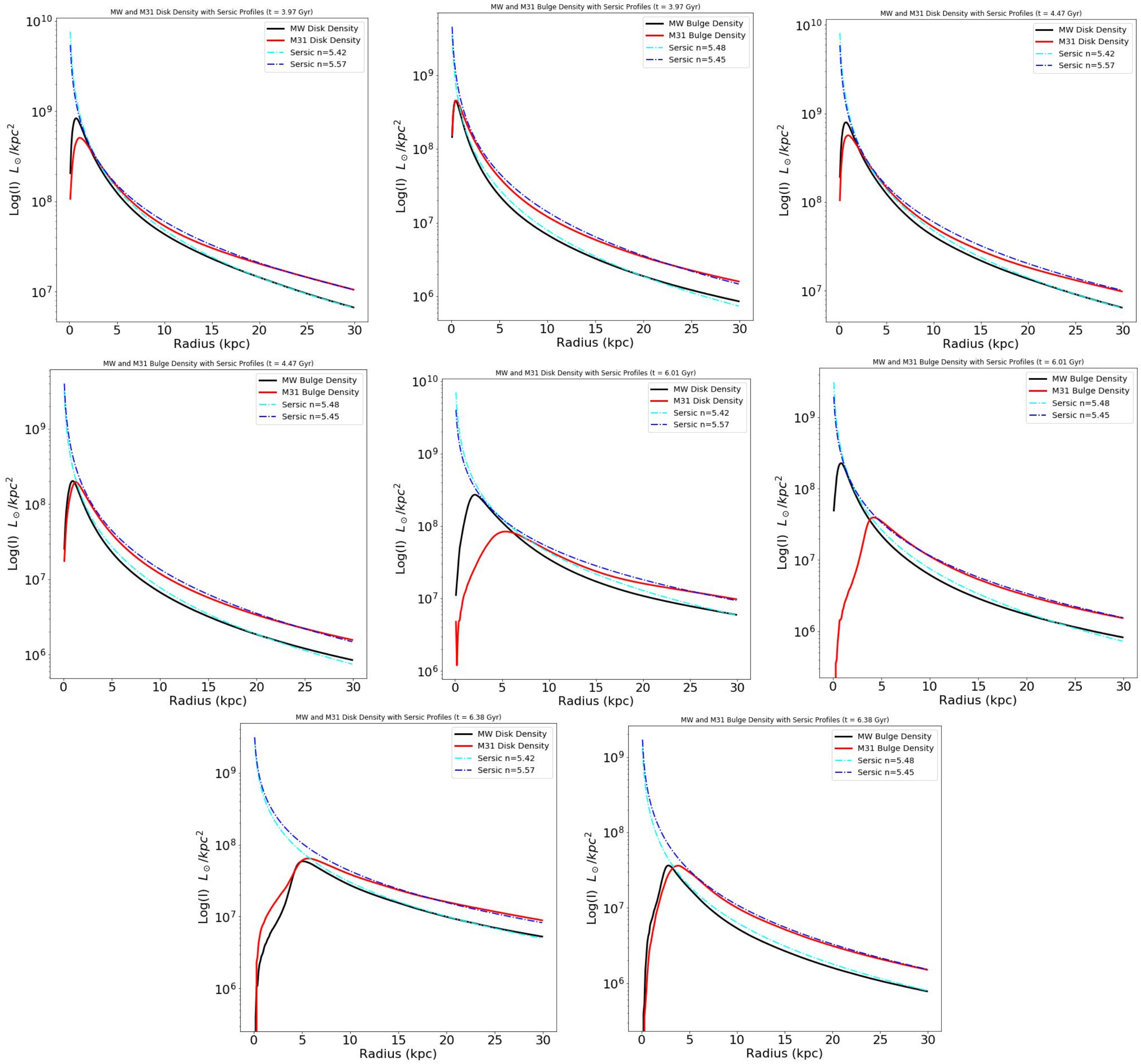

Figure 4: Surface brightness profiles of the Milky Way and M31 galaxies throughout the merger sequence. Times used correspond to times used in van der Marel et al. (2012) for major moments in the sequence. The graphs analogous to t = 3.97 Gyr represent the first close encounter of the two galaxies. The graphs corresponding to t = 4.47 Gyr represent substantial light density disruption as the two galaxies had their first close encounter. The graphs represented by the time t = 6.01 Gyr show the second Milky Way and M31 apocenter. The graphs corresponding to t = 6.38 Gyr represent a moment before final coalescence. All labels and legends are the same as in Figure 3.

described by the serious broadening of the surface brightness profiles in the disk. The surface brightness profile for the bulge densities show obvious spread of light distribution in both the Milky Way and M31 bulges. It appears to show that light has moved from the center and has become more distributed radially outwards, which agrees with the visualization shown of luminous particles seen in Figure 5 of van der Marel et al. (2012) at t = 6.01 Gyr. The fourth set of graphs (bottom left and bottom right) show the most broad distribution of surface brightness. We see that in the disk surface brightness profile, that apparent brightness doesn't fall off as it did for the other graphs. Instead, it remains rather constant, falling slightly with increasing radius. We also notice that the peak for both the disk and bulge apparent brightness begin to match slightly in value, suggesting they have begun the process of final coalescence.

The results of these surface brightness profiles show clear distribution of light concentration during a major merging event and even agree with the results found in van der Marel et al. (2012) for how this distribution might appear.

5. DISCUSSION

Our results outlined in Section 4 support the findings in van der Marel et al. (2012) of how the distribution of luminous particles may look throughout the major merging event. Although the profiles were calculated using de Vaucouleurs' Law they still represent graphically what the distribution of light could look like. We clearly see the interactions gravitationally between these two massive galaxies in the results found in Figure 4. We also see the concentration of light become more spread out throughout the merging event, and that before final coalescence the distribution of light is no longer as strongly biased towards the center.

6. CONCLUSION

In this study we analyzed the distribution of light throughout the major merging event predicted to occur in approximately 4 Gyr between the Milky Way and Andromeda galaxies. The goal was to reinforce the results found in van der Marel et al. (2012) and to show through the use of surface brightness profiles how the concentration of light changed throughout the merger. We observed the distribution of light over 10 billion years with N-body simulations of the three most massive galaxies in the Local Group.

We did find that our profiles agreed with what is found in van der Marel et al. (2012) and that the concentration of luminous objects, do in fact, become less centrally dominant and instead appear to be spread more evenly over a greater radius. Although proper calculations, assuming correct morphological classifications, would need to be completed in the future to get more accurate results. We also have Sersic indices of $n = 5.4$ or greater which would not agree with the Sersic index of spiral galaxies of $n = 1$ (Trujillo et al. 2001), we attribute this to the fact that we had assumed elliptical morphology in our calculations.

While we waver to make conclusions from our case study, our results do still appear to agree with some certainty to the findings in van der Marel et al. (2012). This also seems to suggest that during a major merging event the distribution of light is no longer as centrally dominant. Instead, it is spread out further from the center, which is typical of elliptical galaxies (Brooks & Christensen 2016). If we had used correct calculations for the disk surface brightness profiles, we would be able to compare with even more certainty to the findings in van der Marel et al. (2012). It would be interesting to create surface brightness profiles of other merging events in the future and to see if those results are similar to the ones in this paper. It would also be interesting to expand this to other merger types, for instance, between two elliptical or two irregular galaxies and then compare it to this merging event.

ACKNOWLEDGMENTS

This author would like to thank Dr. Gurtina Besla and Rixin Li for their help with simulation data, plotting software, and general troubleshooting tips among many others. We would also like to thank Trevor Smith for his help in collecting correct snap-numbers that corresponded to the times mentioned in this paper and to Colin Leach for his advice regarding code arrays. We would also like to thank matplotlib (Hunter 2007, DOI: 10.1109/MCSE.2007.55), numpy (van der Walt et al. 2011, DOI: 10.1109/MCSE.2011.37), scipy (Jones et al. 2001-,Open source scientific tools for Python. http://www.scipy.org/), Astropy (Astropy Collaboration et al. 2013; Price-Whelan et al. 2017), and Jupyter Notebooks (The Jupyter Team et al. 2016)

REFERENCES

Brooks, A., & Christensen, C. 2016, Astrophysics and Space Science Library, Vol. 418, Bulge Formation via Mergers in Cosmological Simulations, ed. E. Laurikainen, R. Peletier, & D. Gadotti, 317, doi: 10.1007/978-3-319-19378-6_12

Kormendy, J., & Bender, R. 2019, ApJ, 872, 106, doi: 10.3847/1538-4357/aafdff

Mould, J. 2013, PASA, 30, e027, doi: 10.1017/pas.2013.004

Querejeta, M., Eliche-Moral, M. C., Tapia, T., et al. 2015, A&A, 573, A78, doi: 10.1051/0004-6361/201424303

Ribas, I., Jordi, C., Vilardell, F., et al. 2005, ApJL, 635, L37, doi: 10.1086/499161

Trujillo, I., Graham, A. W., & Caon, N. 2001, MNRAS, 326, 869, doi: 10.1046/j.1365-8711.2001.04471.x

van der Marel, R. P., Besla, G., Cox, T. J., Sohn, S. T., &
Anderson, J. 2012, ApJ, 753, 9,
doi: 10.1088/0004-637X/753/1/9